



Identification of Differentially Expressed Genes (DEGs) by Malachite Green in HepG2 Cells

Youn-Jung Kim¹, Mee Song¹ & Jae-Chun Ryu¹

¹Cellular and Molecular Toxicology Laboratory, Korea Institute of Science and Technology, PO Box 131, Cheongryang, Seoul 130-650, Korea

Correspondence and requests for materials should be addressed to J. C. Ryu (ryujc@kist.re.kr)

Accepted 4 March 2008

Abstract

Malachite Green (MG), a toxic chemical used as a dye, topical antiseptic and antifungal agent for fish, is highly soluble in water, cytotoxic to various mammalian cells and also acts as a liver tumor promoter. In view of its industrial importance and possible exposure to human beings, MG possesses a potential environmental health hazard. So, we performed with HepG2, a human hepatocellular carcinoma cell line, to identify the differentially expressed genes (DEGs) related to toxicity of MG. And we compared gene expression between control and MG treatment to identify genes that are specifically or predominantly expressed by employing annealing control primer (ACP)-based GeneFishing™ method. The cytotoxicity (IC₂₀) of MG was determined above the 0.867 μM in HepG2 cell for 48 h treatment. And the DEGs of MG were identified that 5 out of 6 DEGs were up-regulated and 1 out of 6 DEGs was down-regulated by MG. Also, MG induced late apoptosis and necrosis in a dose dependent in flow cytometric analysis. Through further investigation, we will identify more meaningful and useful DEGs on MG, and then can get the information on mechanism and pathway associated with toxicity of MG.

Keywords: Malachite green, GeneFishing, Differentially expressed genes (DEGs), Apoptosis

Malachite green (MG) belongs to the triphenyl-methane class of dyes, which has been identified as harmful by the WHO/FAO Committee¹. It is used extensively for dyeing wool, jute, cotton, leather, as a

laboratory reagent and as a topical antiseptic². MG is also used as an effective treatment for external fungal and protozoan infections of fish. But MG has been banned because of its cytotoxicity to various mammalian cells³. It has been also reported to cause carcinogenesis, mutagenesis, chromosomal fractures, teratogenicity and respiratory toxicity in mice⁴. Despite the large amount of data on its toxic effects, MG is still used as a parasiticide in aquaculture and other industries⁴.

As shown by Ashra *et al.*⁵, MG is extremely cytotoxic to mammalian cells in culture^{6,7} and induces free radical formation⁸ and malignant transformation³. *N*-demethylated and *N*-oxidized metabolites of MG may induced carcinogenesis by the formation of DNA adduct an abnormal piece of DNA covalently-bonded to a cancer caused by chemical or metabolites⁹. Further in Syrian hamster embryo (SHE) cells,

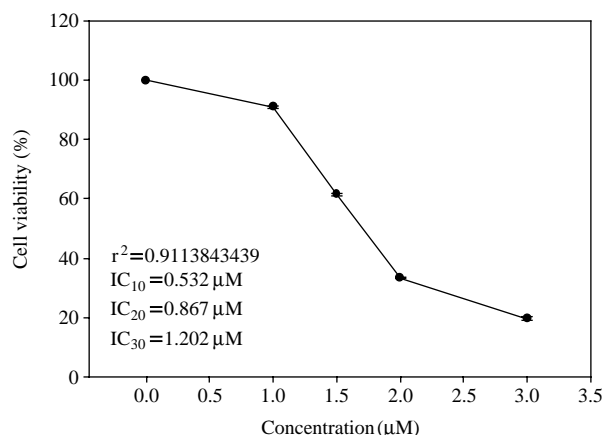


Figure 1. Effect of malachite green on HepG2 cells viability. Dose-response curve assessed after treatment. 6×10^6 cells/mL HepG2 cells of grown for 1 day in 24-well plates were exposed to culture medium. HepG2 cells were treated to various concentrations of malachite green in 24-well plate for 48 h. 75 μL of MTT (4 mg/mL in PBS) solution was added to each well and incubated for 3 h. DMSO solution was added to each well and transfer in 96 well plates. The optical density (O.D.) of the purple formazan product was measured at a wavelength of 540 nm. IC₂₀ value of malachite green was calculated to 0.867 μM at 48 h treatment. Values are expressed as percentage of corresponding controls.

a dose and time dependent induction of apoptosis increased by MG. And the overexpression of p53 and bcl-2 related to oncogenesis and tumor progression induces apoptosis by MG^{10,11}. And also, MG also induced G2/M arrest in dose-dependent manner⁵. Monisha Sundarajan *et al.*¹² have early reported that MG has promoter effects on development of hepatic pre-neoplastic lesion in rats^{6,13,14}. However, the information available on the liver tumor promoting effects of MG, much still remains unknown regarding the possible mechanism (s) of tumor promotion by this compound.

This study examined whether MG has an influence on the expression of mRNA in HepG2, the human hepatocellular carcinoma cell line. The identification of differentially expressed genes (DEGs) induced by MG may assist in the identification of potential bio-

marker and may understand molecular toxicological mechanisms in HepG2 cells. So, we performed the GeneFishingTM techniques incorporating an annealing control primer, which has specificity to the template and allows only real products to be amplified¹⁵, for identification of DEGs on MG exposure. And we also suggest that one of toxic mechanism on MG may be the induction of apoptosis. Thus, we have measured whether MG induces apoptosis using flow cytometry assay and it affects the expression of apoptosis-related genes using real time RT-PCR.

Cytotoxicity of Malachite Green in Human HepG2 Cells

Relative survival of HepG2 cells following exposure to a range of concentrations of MG was determined by MTT assay. The survival percentage relative to sol-

Table 1. Sequence similarities and characterization of differentially expressed transcripts in the cell by malachite green exposure.

DEG No.	Gene symbol	Accession No.	Sequence homology search	Homology (<i>Homo sapiens</i>)
Up 1	AGXT	NM_000030	Homo sapiens alanine-glyoxylate aminotransferase (oxalosis I; hyperoxaluria I; glycolicaciduria; serine-pyruvate aminotransferase) (AGXT), mRNA	387/388 (99%)
	PAGA	X53414	Human mRNA for peroxisomal L-alanine:glyoxylate aminotransferase	387/388 (99%)
Up 2	RPS20	BC007507	Homo sapiens ribosomal protein S20, mRNA	347/347 (100%)
Up 3	GDF15	AB000584	Growth differentiation factor 15	371/371 (100%)
	MIC-1	AF019770	Homo sapiens macrophage inhibitory cytokine-1 (MIC-1), mRNA	371/371 (100%)
Up 4	WDR59	NM_030581	Homo sapiens WD repeat domain 59 (WDR59), mRNA	204/204 (100%)
	FP977	AF370390	Homo sapiens FP977, mRNA	204/204 (100%)
Up 5	KB-EST BPS7	DT219620	KB-EST0004704 BPS7 Homo sapiens cDNA, mRNA sequence	330/330 (100%)
	43 M1b1a	EF060354	Homo sapiens isolate 43_M1b1a (Tor259) mitochondrion, complete genome	330/330 (100%)
Up 6	ULK1	XM001133335	Homo sapiens unc-51-like kinase1 (<i>C. elegans</i>) (ULK1), mRNA	478/478 (100%)
Up 7	COX5A	AK026623	Homo sapiens nuclear-encoded mitochondrial cytochrome c oxidase Va subunit, mRNA	482/483 (99%)
Down 1	RS3K	DQ862537	Homo sapiens isolate RS3K mitochondrion, complete genome	412/413 (99%)
Down 2	YAN0637	AF465980	Homo sapiens clone YAN0637 mitochondrion, partial genome	593/593 (100%)
Down 3	3719	DQ862536	Homo sapiens isolate 3179 mitochondrion, complete genome	637/637 (100%)
Down 4	B2-1-06	DQ282439	Homo sapiens isolate B2-1-06 mitochondrion. Complete genome (cytochrome c oxidasesubunit1)	655/655 (100%)

All genes identified in the present study had been submitted to GenBank and assigned accession numbers. Homology is a BLAST search for sequence similarity with *Homo sapiens* in NCBI GenBank.

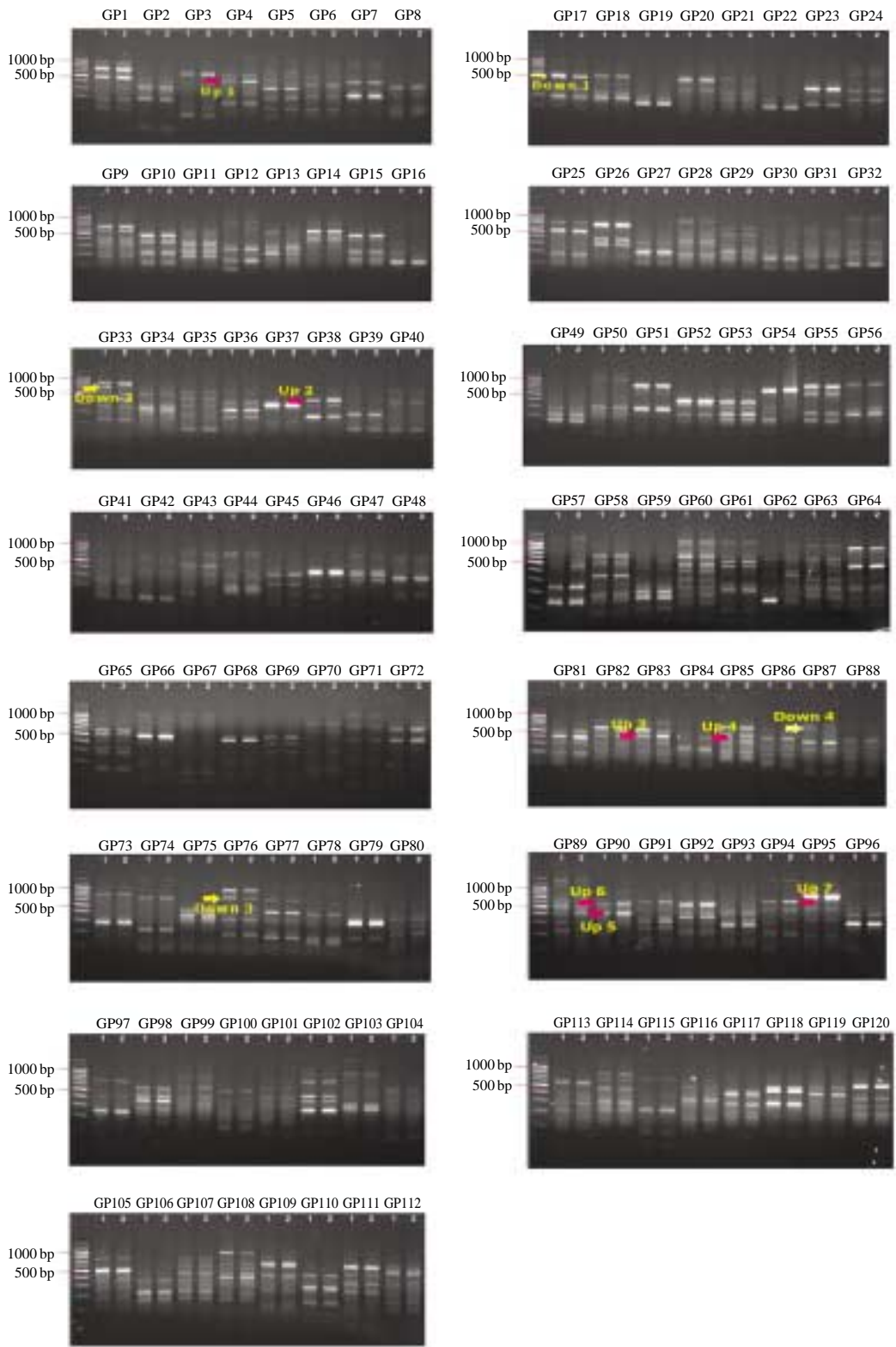


Figure 2. Agarose gel pictures showing the amplified cDNA products obtained from head portions from control and treated samples with dT-ACP2/arbitrary 1-120ACPs in differentially expressed genes (DEGs) kit. The numbers with arrows indicate differential expressed bands between control and treated samples (1: control; 2: treatment). Bands were excised from the gel for sequencing.

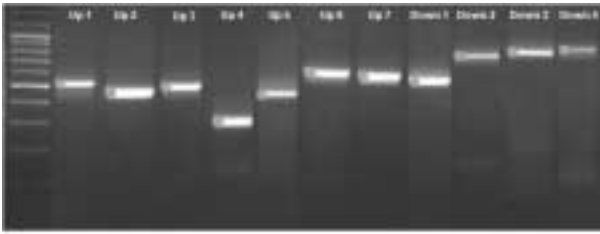


Figure 3. Re-amplification result. The extracted DNA fragments were directly sequenced.

vent control (DMSO) was determined as a percentage of OD value measured after treatment. Based on the results of MTT assay, 20% inhibitory concentration (IC_{20}) of MG was calculate. Dose dependent cell viability curves were obtained after 48 h of exposure to MG in HepG2 cells as shown Figure 1. MG reduced cell viability gradually at increasing concentrations. The IC_{20} for MG was $0.867 \mu\text{M}$ (Figure 1). So, we used this concentration for GeneFishingTM method.

Differentially Expressed Amplified Genes (DEGs) in Malachite Green-treated Cells

To identify genes that are specifically or predominantly expressed in the MG treated HepG2 cells, we compared the mRNA expression profiles of vehicle treated cells and $0.867 \mu\text{M}$ MG treated cells. To do this, the mRNAs from both types of cells were extracted and subjected to ACP RT-PCR analysis using a combination of 120 arbitrary primers and two anchored oligo (dT) primers (dT-ACP 1 and dT-ACP 2). This method is depicted in the Materials and Methods. Among hundreds of amplicons displayed, 11 amplicons that expressed differentially were excised from the gels. Up1-7 were markedly up-regulated in the MG treated group compared with the control group. And Down 1-4 were down-regulated in the MG treated group compared with the control group (Figure 2). Figure 3 represent re-amplification of 11 amplicons that the extracted DNA fragments were directly sequenced for analysis and numbered as 11 DEGs (Up 1-7, Down 1-4). The identity, GenBank accession number and homology of differentially expressed transcripts are summarized in Table 1. A BLAST search for sequence similarity in NCBI GenBank revealed 11 DEGs. AGXT (Up 1, Alanine-glyoxylate aminotransferase), RPS20 (Up 2, ribosomal protein S20), GDF15 (Up 3, Growth differentiation factor 15), WDR59 (Up 4, WD repeat domain 59), KB-EST BPS7 (Up 5, KB-EST0004704 BPS7 Homo sapiens cDNA), ULK1 (Up 6, unc-51-like kinase1 (*C. elegans*)), COX5A (Up 7, cytochrome *c* oxidase su-

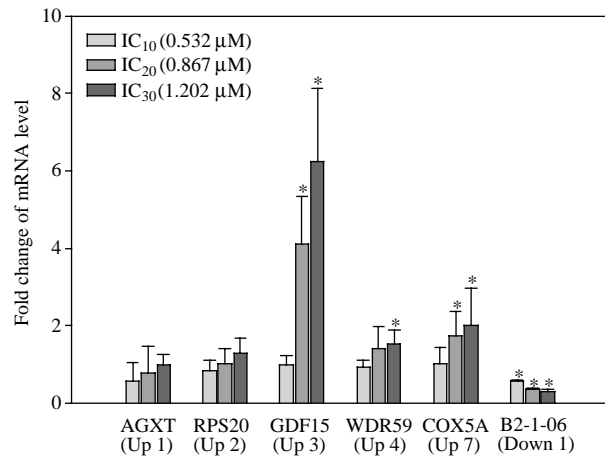


Figure 4. Confirmation by quantitative real-time reverse transcription-polymerase chain reaction (RT-PCR) of mRNA expression patterns of six genes. *: 1.5 fold change.

bunit Va), RS3K (Down 1, RS3K mitochondrion), YAN0637 (Down 2, YAN0637 mitochondrion), 3719 (Down 3, 3719 mitochondrion) and B2-1-06 (Down 4, cytochrome *c* oxidase subunit1) showed significant similarities (99-100%) with sequences from *Homo sapiens*. All genes identified in the present study had already been submitted to GenBank and assigned accession numbers.

Confirmation of DEGs Expression by Real-time Reverse Transcriptase-Polymerase Chain Reaction

To confirm genes that are specifically or predominantly expressed in the MG treated HepG2 cells, we used real-time RT-PCR. So, we compared the mRNA expression levels of vehicle treated cells with MG of each concentration ($0.532 \mu\text{M}$, $0.867 \mu\text{M}$, $1.202 \mu\text{M}$). The expression patterns of AGXT (Up 1), RPS20 (Up 2), GDF15 (Up 3), WDR59 (Up 4), COX5A (Up 7) and B2-1-06 (Down 4) were confirmed by RT-PCR (Figure 4). However, the RT-PCR data of Up 5, 6 and Down 1, 2, 3 were not consistent with GeneFishing data. Sequence-specific primers were designed to amplify products with lengths ranging from 80 to 200 bp. To normalize the efficiency of RT-PCR reaction, GAPDH was used as an internal standard. The expression of this housekeeping gene did not vary across different conditions. The RT-PCR assay revealed that, in accordance with the ACP differential display, AGXT, RPS20, GDF15, WDR59, and COX5A were highly expressed in MG treated cells compared to control cells, whereas B2-1-06 was less expressed after MG treated cells (Figure 4).

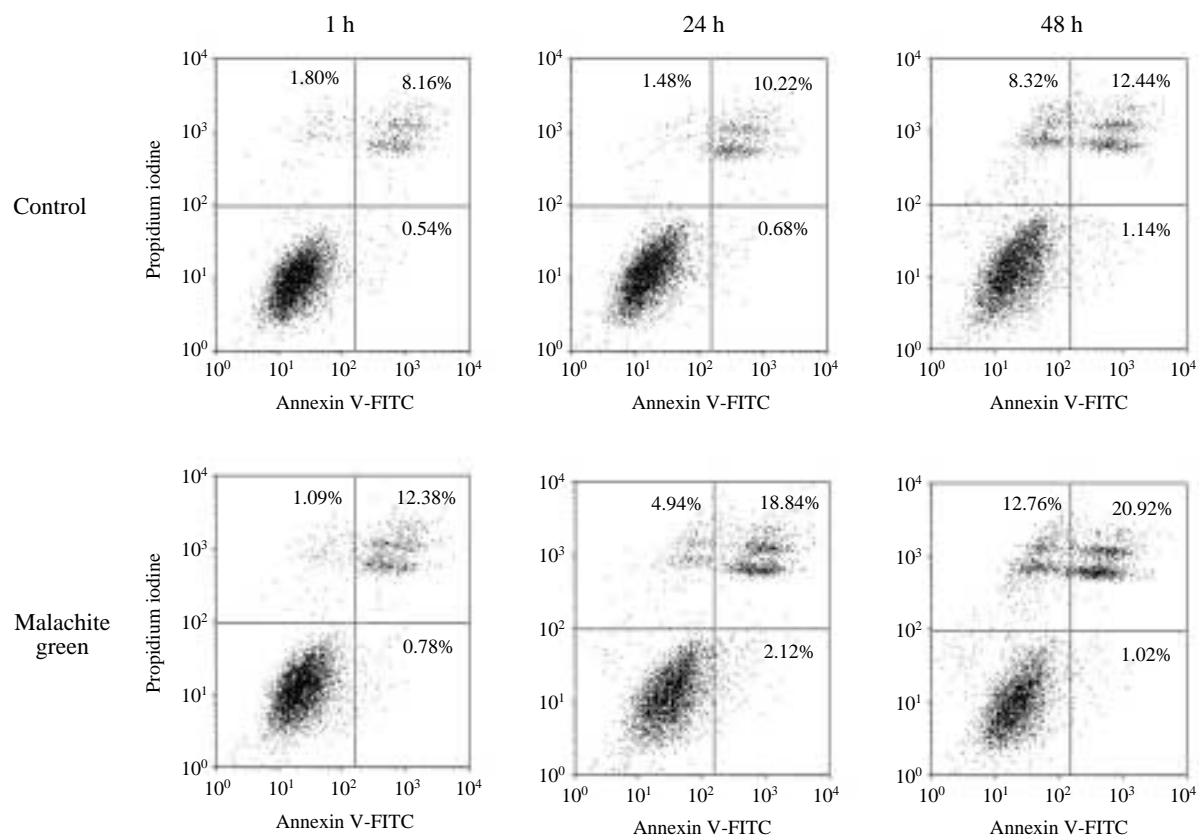


Figure 5. The effect of malachite green on either early or late stage of HepG2 apoptosis as detected by flow cytometry. HepG2 were incubated in DMEM supplemented with 10% FBS without (control) or with 0.867 μM malachite green. After 1 h, 24 h and 48 h, the cells were harvested, stained with Annexin V-FITC and propidium iodide, and analysed by flow cytometry. Data are expressed as % of Annexin V-FITC and PI-negative cells (early state of apoptosis) and as % of Annexin V-FITC and PI-positive cells (late stage of apoptosis or necrosis). Diagrams of Annexin V/PI flow cytometry in a representative experiment are presented the graphs. The lower right quadrants represent the cells in the early stage of apoptosis. The upper right quadrants contain the cells in the late stage of apoptosis or necrosis.

Effect of Malachite Green on Late Apoptosis and Necrosis

In order to check whether MG induce apoptosis in HepG2 cells or not, the presence of apoptotic HepG2 cells using the flow cytometry assays was confirmed by double staining with propidium iodide and Annexin-V-FITC. Untreated controls maintained a relatively uniform distribution throughout the experiment. As shown by Figure 5, MG did not influence significantly the proportions of early apoptotic cells. But continuous treatment with 0.867 μM MG increased dramatically the number of late apoptotic cells and necrotic cells. The number of late apoptotic cells increased slightly at 1 h, from 8.16 to 12.38%, and dramatically at 24 h and 48 h, from 10.22 to 18.84% and from 12.44 to 20.92%, respectively. At the same time, the number of necrotic cells increased after 24 h and 48 h, from 1.48 to 4.94% and from 8.32 to 12.76 %, respectively. There was a clear increase in the

number of necrotic cells and late apoptosis, which reached approximately 34% of the cell population after 48 h.

The GDF15 expression can regulate p53 inducing up-regulated bax leading to release cytochrome *c*. The cytochrome *c*, apaf1 and caspase 3 form a complex and may induce apoptosis. As stated above, the expression patterns of apoptosis related genes such as TNF, p53, caspase 3, and bax were confirmed by quantitative real-time reverse transcription-polymerase chain reaction (Figure 6). While caspase 3 and bax are not changing in expression, TNF and p53 increased in dose-dependent manner by MG.

Discussion

Understanding molecular mechanisms of MG in HepG2 cell requires investigation of gene expression

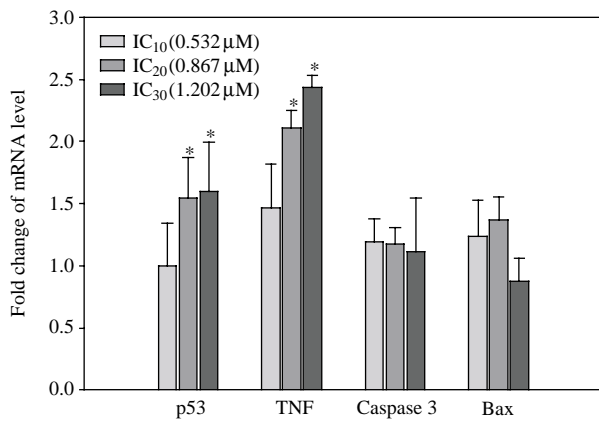


Figure 6. The expression patterns of apoptosis related genes were confirmed by quantitative real-time reverse transcription-polymerase chain reaction (RT-PCR). *: 1.5 fold change. Sequence-specific primers used for real-time PCR are forward primer for TNF 5'-CCAGGGACCTCTCTCTAATCA-3', reverse primer for TNF 5'-GCTACAGGCTTGTCACTCGG-3', forward primer for p53 5'-TCAACAAGATGTTTTGCCAACTG-3', reverse primer for p53 5'-ATGTGCTGTGACTGTGTAGATG-3'; forward primer for caspase 3 5'-AGAACTGGACTGTGGCATTGAG-3', reverse primer for caspase 3 5'-ATGTGCTGTGACTGCTTGTAGATG-3'; forward primer for bax 5'-CCTTTTCTACTTTGCCAGCAAAC-3', reverse primer for bax 5'-GAGGCCGTCCCAACCAC-3'.

profiles to identify DEGs and to further characterize their function. To detect DEGs that are transcribed at low levels, highly specific PCR amplification is required. Several RT-PCR methods have been used to identify novel genes or expressed sequences. DEGs discovery method such as microarray, differential display (DD-PCR) and serial analysis of gene expression (SAGE) are simple and fast but suffering from high false positive rate, low reproducibility and low sensitivity. Unlike existing DEGs discovery method, ACP-base PCR method involves an ACP that has a unique tripartite structure in that its distinct 30- and 50-end portions are separated by a regulator facilitates the identification of DEGs from samples displaying low levels without generating false positives^{9,16-18}. In this study, GeneFishingTM method applied to the ACP-based PCR method was employed in order to find DEGs responded by the effect of MG in HepG2 cells.

Using dT-ACP2 (reverse primer) and 120 arbitrary ACPs (forward primer) for amplification, we displayed hundreds of cDNA comparative analysis. The majority of differentially expressed cDNA bands were shown to respond when MG was applied to HepG2 cells (Figure 2). Subsequently, 6 DEGs of MG specific cDNA bands were identified, and transcripts confirmed by real-time quantitative RT-PCR. Sequence

analysis results represent that all cloned ESTs share significant similarity with human genes available in GenBank. A total of 6 DEGs exhibited significantly higher sequence similarity (99-100%) with the coding regions of known genes. We identified genes for growth differentiation factor 15, Alanine-glyoxylate aminotransferase, cytochrome *c* oxidase subunit Va, ribosomal protein S20, WD repeat domain 59 were up-regulated, whereas a gene for cytochrome *c* oxidase subunit I was down-regulated by MG. Alanine-glyoxylate aminotransferase (AGXT) expressed in peroxisomes and mitochondria of hepatocytes is an intermediary metabolic enzyme that catalyses the transamination of glyoxalate to glycine using alanine. AGXT may have an important role in gluconeogenesis in mitochondria and glyoxalate detoxification in peroxisomes. The detoxification of glyoxalate influenced on overproduction of oxalate induces nephrocalcinosis¹⁹. The ribosomal protein S20 (RPS20) encodes a component of the 60S ribosomal subunit. Since ribosomal proteins and rRNA regulate protein synthesis, the effect of ribosomal biogenesis is one of the possible mechanisms which the disruption of cellular growth control results in increased proliferation. Therefore, Up-regulated ribosomal proteins and rRNA have influence on the formation of cancer cells display increased metabolism and protein synthesis²⁰. WD repeat domain 59 (WDR59) is reported that this gene expressed in cancerous cervical epithelial cells not found in normal cervical epithelial cells²¹.

The Growth differentiation factor 15 (GDF15) gene induced in hepatocytes by chemical injury and carcinogen exposure is a member of the TGF- β superfamily of growth and differentiation factors and a transcriptional target gene for p53²². Zimmers *et al.* demonstrate that GDF-15 expression in mice is an immediate early response to liver injury that can occur through p53 independent pathways²³. Also, GDF-15 expression increase after administration of TNF and interleukin-6 (IL-6).

We found DEGs (Up 7: cytochrome *c* oxidase Va subunit (COX5A) and Down 4: Cytochrome *c* oxidase subunit 1 (B2-1-06) related to mitochondrial DNA. MG accelerated a dissipation of mitochondrial membrane potential, accompanied by mitochondrial swelling, resulting in mitochondrial permeability transition. The mitochondrial permeabilization was caused by respiratory inhibition, attributable to cytochrome *c* release, and was caused by the oxidation of NAD (P)H promoted by MG²⁴. Also, COX5A increases Bax and caspase 3 gene expression. COX genes encoded in nuclear may regulate cytochrome *c* transport. Therefore, COX5A and B2-1-06 may lead to release of cytochrome *c*, and then a change of membrane

potential in the mitochondrial leads to apoptosis²⁵.

Therefore, we hypothesize that when MG treated in hepatocytes, TNF and IL-6 may regulate the expression of GDF15. The GDF15 expression can regulate p53 inducing up-regulated bax leading to release cytochrome *c*. The cytochrome *c*, apaf1 and caspase 3 form a complex and may induce apoptosis. When the expression patterns of apoptosis related genes such as TNF, p53, caspase 3, and bax confirmed by quantitative real-time RT-PCR (Figure 6), TNF and p53 increased in dose-dependent manner by MG. And, we also confirmed that MG induced late apoptosis and necrosis in dose-dependent manner from FACS analysis results.

Therefore, we can hypothesize that MG may induce necrosis and late apoptosis increased by the expression of TNF, GDF15 and p53, in sequence. Through these results, we can get the information on the associated mechanism and pathway with toxicity by MG exposure.

Methods

Materials

MG oxalate salt, sodium bicarbonate and 3-(4,5-dimethylthiazol-2-yl)-2,5-diphenyl-tetrazolium bromide (MTT) was purchased from Sigma (USA). Dulbecco's Modified Eagle Medium (DMEM), fetal bovine serum (FBS), sodium pyruvate, penicillin, streptomycin were the products of GIBCO BRL (Grand Island, NY, USA). All other chemicals used were of analytical grade or the highest grade available.

Cell Lines and Culture

HepG2 cell line was purchased from Korean Cell Line Bank and maintained in a humidified atmosphere of 5% CO₂ and 95% air at 37°C. The culture medium was 90% DMEM with 1 mM sodium pyruvate, 0.1% sodium bicarbonate with 10% fetal bovine serum (FBS) plus penicillin, streptomycin. The cells had been maintained by 3-4 day passages.

Cytotoxicity (Cell Growth Inhibition)

Cytotoxicity of cells was checked by MTT assay. For the determination of cell cytotoxicity, 6×10^6 HepG2 cells were treated to various concentrations of MG in 24-well plate for 48 h. 75 μ L of MTT (4 mg/mL in PBS) solution was added to each well and incubated for 3 h. DMSO solution was added to each well and transfer in 96 well plates. The optical density (O.D.) of the purple formazan product was measured at a wavelength of 540 nm. Cell viability of treated chemical was related to controls that were treated

with the solvent. The 20% inhibitory concentration (IC₂₀) of a particular agent was defined as that concentration that causes a 20% reduction in the cell number versus the untreated control. The IC₂₀ values were directly determined from the semi-logarithmic dose-response curves.

GeneFishing™ Reverse Transcription-Polymerase Chain Reaction

Total RNAs from HepG2 cells treated to MG and vehicle were isolated using Trizol (GibcoBRL) and purified with RNeasy mini kit (Qiagen, Valencia, CA, USA). Reverse transcription (RT) was conducted using the GeneFishing™ DEG kits (Seegene, Seoul, South Korea) as follows; 3 μ g of the extracted RNAs were put into a tube containing RNase-free water and 10 μ M dTACP1 with a final volume of 9.5 μ L using a DNA Thermal Cycler 9600 (Perkin Elmer, Foster City, CA, USA). Equal amounts of RNA were compared with identify differentially expressed bands between the samples. The mixture was incubated at 80°C for 3 min and spun briefly after chilling on ice. Twenty μ L of reaction solution, consisting of 5X RT buffer, 2 mM dNTP, RNase inhibitor, and M-MLV RT (Promega, Madison, WI, USA), was added to the mixture. The tube was incubated at 42°C for 90 min, heated at 94°C for 2 min, chilled on ice and spun briefly. The synthesized first-strand cDNA was diluted by adding 80 μ L of RNase-free water. The cDNA samples were stored at 20°C until use. Polymerase chain reaction (PCR) amplification was conducted using the same GeneFishing™ DEG kits (Seegene) in 50 μ L of reaction solution, consisting of 10X buffer without MgCl₂, 25 mM MgCl₂, 5 μ M arbitrary ACPs, 10 μ M dTACP2, 2 mM dNTP, 2.5 U Taq DNA polymerase (Genecraft, Ludinghausen, Germany), and 50 ng of first-strand cDNA, using a DNA Thermal Cycler 9600 (Perkin Elmer). This kit comprises 20 different arbitrary annealing control primers. The thermal cycler was preheated to 94°C before the tubes were placed in it. The program of PCR amplification was as follows; 1 cycle at 94°C for 5 min, 50°C for 3 min, and 72°C for 1 min, 40 cycles at 94°C for 40 s, 65°C for 40 s, and 72°C for 40 s, and 72°C for 5 min. The DNA fragments produced by PCR were separated by electrophoresis on a 2% agarose gel. The bands were photographed using polaroid film under ultraviolet light after ethidium bromide staining and analyzed by a densitometry (Pharmacia, Uppsala, Sweden).

Direct Sequencing

The differentially expressed band was re-amplified and extracted from the gel by using the GENCL-EAN® II Kit (Q-BIO gene, Carlsbad, CA, USA), and

Table 2. Sequence-specific primers used for real-time PCR.

DEG No.	Accession No.	Gene symbol		Primer	Product size (bp)
Up 1	NM_000030	AGXT	F R	ATCAGGAGCAAACAGACCCTGCAA GCTCATTTGGAAGGCACTGGGTTT	176
Up 2	BC007507	RPS20	F R	AAGGACCAGTTCGAATGCCTACCA TTCCACCTCAACTCCTGGCTCAAT	188
Up 3	AB000584	GDF15	F R	GTTAGCCAAAGACTGCCACTGCAT TGTCTCAGGAACCTTGAGCCATT	117
Up 4	NM_030581	WDR59	F R	AGGAGCGGAAATCAAGACGATGGA ATTTGTGAACAGGCAGGAGGCAAG	123
Up 7	AK026623	COX5A	F R	CAAAGTGTAACCGCATGGA TCCAGGTAACCTGTTACACTCAA	76
Down 4	DQ282439	B2-1-06	F R	TAGGTGGCCTGACTGGCATTGTAT TTTGGCGTAGGTTTGGTCTAGGGT	185
		GAPDH	F R	TGCACCACCAACTGCTTAGC GGCATGGACTGTGGTCATGA	

directly sequenced with ABI PRISM® 3100-*Avant* Genetic Analyzer (Applied Biosystems, Foster City, CA, USA).

Real-time Reverse Transcriptase-Polymerase Chain Reaction Confirmation

The mRNA levels for the interested genes in HepG2 cells were analyzed by quantitative real time RT-PCR using a Bio-Rad iCycler system (Bio-Rad, Hercules, CA, USA). The mRNAs were reverse-transcribed into cDNAs by using an Omniscript RT kit (Qiagen). The primer specificity was tested by running a regular PCR for 40 cycles at 95°C for 20 s and 60°C for 1 min, and followed by an agarose gel electrophoresis. The real time RT-PCR was performed by using a SYBR supermix kit (Bio-Rad), and running for 45 cycles at 95°C for 20 s and 60°C for 1 min. The PCR efficiency was examined by serially diluting the template cDNA and the melting curve data were collected to check the PCR specificity. Each cDNA sample was triplicated and the corresponding no-RT mRNA sample was included as a negative control. The Glyceraldehyde-3-phosphate dehydrogenase (GAPDH) primer was included in every plate to avoid sample variations. The mRNA level of each sample for each gene was normalized to that of the GAPDH mRNA. Relative mRNA level was presented as $2^{-(Ct/GAPDH - Ct/gene\ of\ interest)}$. All data shown were the mean \pm SD of three separate experiments. Primers used for quantitative real time RT-PCR were as Table 2.

Analysis of Apoptosis by Flow Cytometry

The *ApoScan*TM Annexin V-FITC apoptosis detection Kit (BioBud, Korea) was used to detect apoptosis

by flow cytometry. HepG2 cells (2×10^6 cells/mL) were plated onto 60 mm dishes and incubated with MG for 1 h, 24 h, 48 h. HepG2 cells were trypsinized, harvested, and resuspended (1×10^6 cells/mL) in DMEM. HepG2 cells were washed in cold-buffered saline (PBS) and pelleted by centrifugation at $1,000 \times g$ for 5 min. They were then resuspended in a $1 \times$ binding buffer (500 μ L) and incubated with 1.25 μ L of Annexin V-FITC (200 μ g/mL) at room temperature for 15 min. The cells were resuspended in 500 μ L of a $1 \times$ binding buffer and then cell suspensions were stained with 10 μ L of PI (30 μ g/mL) at 4°C in the dark. The fluorescence was determined using a FACScan flow cytometer (Becton-Dickinson, Mountain View, CA, USA). A computer system (CellQuest Pro, Becton Dickinson) was used for data acquisition and analysis. Data for 5000 events were stored.

Acknowledgements

This subject is supported by the Korea Research Foundation grants from Korea Ministry of Environment as “The Eco-technopia 21 project”, KIST Core-Competence Program to Ryu, J. C. of the Republic of Korea.

References

1. WHO, World Health Organisation. Technical Report Series No. 309. Geneva, Switzerland (1965).
2. Windholz, M., Budhavani, S., Bluemetti, R. F. & Otterbein, E. S. The Merck Index (10th ed.), Merck and Co., Inc., Rahway, NJ 813 (1983).

3. Rao, K. V. K., Mahudawala, D. M. & Redkar, A. A. Malignant transformation of Syrian hamster embryo (SHE) cells in primary culture by malachite green: transformation is associated with abrogation of G2/M checkpoint control. *Cell Biol Int* **22**:581-589 (1998).
4. Srivastava, S., Sinha, R. & Roy, D. Toxicological effects of malachite green. *Aquat Toxicol* **66**:319-329 (2004).
5. Ashra, H. & Rao, K. V. Elevated phosphorylation of Chk1 and decreased phosphorylation of Chk2 are associated with abrogation of G2/M checkpoint control during transformation of Syrian hamster embryo (SHE) cells by Malachite green. *Cancer Lett* **237**: 188-198 (2006).
6. Fernandes, C., Lalitha, V. S. & Rao, K. V. Enhancing effect of malachite green on the development of hepatic pre-neoplastic lesions induced by N-nitrosodiethylamine in rats. *Carcinogenesis* **12**:839-845 (1991).
7. Panandiker, A., Fernandes, C. & Rao, K. V. K. The cytotoxic properties of malachite green are associated with the increased demethylase, arylhydrocarbon hydroxylase and lipid peroxidation in primary cultures of Syrian hamster embryo cells. *Cancer Lett* **67**: 93-101 (1992).
8. Panandiker, A., Maru, G. B. & Rao, K. V. K. Dose effects of malachite green on free radical formation, lipid peroxidation and DNA damage in Syrian hamster embryo cells and their modulation by antioxidants. *Carcinogenesis* **15**:2445-2448 (1994).
9. Culp, S. J. *et al.* Toxicity and metabolism of malachite green and leucomalachite green during short-term feeding to Fischer 344 rats and B6C3F1 mice. *Chem Biol Interact* **122**:153-70 (1999).
10. Rao, K. V., Mahudawala, D. M. & Redkar, A. A. Malachite green induced malignant transformation of Syrian hamster embryo (SHE) cells in primary culture: transformation is associated with enhanced expression of altered p53, bcl-2 and decreased sensitivity to apoptosis. *J Exp Clin Cancer Res* **19**:89-98 (2000).
11. Rao, K. V., Mahudawala, D. M. & Redkar, A. A. Abrogation of cell cycle checkpoint controls during malignant transformation of syrian hamster embryo cells is associated with decreased sensitivity to apoptosis. *J Environ Pathol Toxicol Oncol* **20**:177-188 (2001).
12. Mahudawala, D. M., Redkar, A. A., Wagh, A., Gladstone, B. & Rao, K. V. Malignant transformation of Syrian hamster embryo (SHE) cells in culture by malachite green: an agent of environmental importance. *Indian J Exp Biol* **37**:904-918 (1999).
13. Rao, K. V. K. & Fernandes, C. Progressive effects of malachite green at varying concentrations on the development of N-nitrosodiethylamine induced hepatic preneoplastic lesions in rats. *Tumori* **82**:280-286 (1996).
14. Fernandes, C. & Rao, K. V. Dose related promoter effect of metanil yellow on the development of hepatic pre-neoplastic lesions induced by N-nitrosodiethylamine in rats. *Indian J Med Res* **9**:100-140 (1994).
15. Hwang, I. T. *et al.* Annealing control primer system for improving specificity of PCR amplification. *Biotechniques* **35**:1180-1184 (2003).
16. Kim, Y. J., Kwak, C. I., Gu, Y. Y., Hwang, I. T. & Chun, J. Y. Annealing control primer system for identification of differentially expressed genes on agarose gels. *Biotechniques* **36**:424-430 (2004).
17. Hwang, K. C., Lee, H. Y., Cui, X. S., Kim, J. H. & Kim, N. H. Identification of maternal mRNAs in porcine parthenotes at the 2-cell stage: a comparison with the blastocyst stage. *Mol Reprod* **70**:314-23 (2005).
18. Kim, Y. J., Kim, M. S. & Ryu, J. C. Genotoxicity and identification of differentially expressed genes of formaldehyde in human jurkat cells. *Mol Cell Toxicol* **1**:230-236 (2005).
19. Koul, S., Johnson, T., Pramanik, S. & Koul, H. Cellular transfection to deliver alanine-glyoxylate aminotransferase to hepatocytes: a rational gene therapy for primary hyperoxaluria-1 (PH-1). *Am J Nephrol* **25**:176-182 (2005).
20. De Bortoli M. *et al.* Medulloblastoma outcome is adversely associated with overexpression of EEF1D, RPL30, and RPS20 on the long arm of chromosome 8. *BMC Cancer* **6**:223-235 (2006).
21. Sun de J. *et al.* Endothelin-3 growth factor levels decreased in cervical cancer compared with normal cervical epithelial cells. *Hum Pathol* **38**:1047-1056 (2007).
22. Osada, M. *et al.* A p53-type response element in the GDF15 promoter confers high specificity for p53 activation. *Biochem Biophys Res Commun* **354**:913-918 (2007).
23. Zimmers, T. A. *et al.* Growth differentiation factor-15: induction in liver injury through p53 and tumor necrosis factor-independent mechanisms. *J Surg Res* **130**:45-51 (2006).
24. Kowaltowski, A. J., Turin, J., Indig, G. L. & Vercesi, A. E. Mitochondrial effects of triarylmethane dyes. *J Bioenerg Biomembr* **31**:581-590 (1999).
25. Cui, X. S., Li, X. Y., Jeong, Y. J., Jun, J. H. & Kim, N. H. Gene expression of cox5a, 5b, or 6b1 and their roles in preimplantation mouse embryos. *Biol Reprod* **74**:601-610 (2006).